

Transfer function method for frequency response and damping effect of multilayer PCLD on cylindrical shell

Q Qiu, Z P Fang, H C Wan and L Zheng

The State Key Laboratory of Mechanical Transmission, Chongqing University,
Chongqing, China

E-mail: zling@cqu.edu.cn

Abstract. Based on the Donnell assumptions and linear visco-elastic theory, the constitutive equations of the cylindrical shell with multilayer Passive Constrained Layer Damping (PCLD) treatments are described. The motion equations and boundary conditions are derived by Hamilton principle. After trigonometric series expansion and Laplace transform, the state vector is introduced and the dynamic equations in state space are established. The transfer function method is used to solve the state equation. The dynamic performance including the natural frequency, the loss factor and the frequency response of clamped-clamped multi-layer PCLD cylindrical shell is obtained. The results show that multi-layer PCLD cylindrical shell is more effective than the traditional three-layer PCLD cylindrical shell in suppressing vibration and noise if the same amount of material is applied. It demonstrates a potential application of multi-layer PCLD treatments in many critical structures such as cabins of aircrafts, hulls of submarines and bodies of rockets and missiles.

1. Introduction

The Passive Constrained Layer Damping (PCLD) is composed of host shell, visco-elastic material (VEM) layer and constrained layer. In the past decades, it has been an effective way to suppress the vibration and noise in structures. Because the tensile deformation in VEM is limited by the constrained layer, the shear deformation in VEM is increased, more vibration energy is dissipated by means of VEM, vibration and noise in structures is thus reduced significantly. The PCLD is widely used in aviation, aerospace, submarine, vehicle, etc due to simple structure, low cost, high reliability and effectiveness in a wide temperature and frequency range.

In this field, the pioneer work (Kerwin, 1959) derived an expression for an effective, complex, flexural stiffness of the three-layer beams with damping core layer. By extending Kerwin's work, a sixth order partial differential equation of motion governing the transverse displacement of a sandwich beam with arbitrary boundary conditions was developed and a theoretical foundation for PCLD beams was established (Mead et al. 1969). The influence of treatment location on the vibration characteristic of PCLD beams has been investigated (Yeh et al. 2006). By developing a dynamic model of a PCLD laminated rectangular plate, the Galerkin Element Method (GEM) was proposed (Zhang et al. 2000); The GEM is more accurate and effective than traditional Finite Element Method (FEM). A mathematical model for PCLD plate based on the thick plate theory was developed (Chen et al. 2002); Their research suggested that the maximum vibration energy dissipation in PCLD plate can be achieved as the thickness of Constrained Layer (CL) is twice of the thickness of VEM.



The work on the cylindrical shell with PCLD treatment has attracted many researches in the recent decades. The solution mainly included FEM, analytical method and semi-analytical method. FEM has been widely applied due to its flexible and available for arbitrary geometry and boundary conditions. A conventional finite element model for the vibration and damping analysis of a cylindrical shell with a visco-elastic core was developed and the influence of geometric parameters and VEM's shear modulus on suppressing vibration was investigated (Ramesh et al. 1994). The dynamic characteristic of a cylindrical shell with partial PCLD treatment (Wang et al. 2004) was analyzed using a finite element model. A finite element model of the cylindrical shell with fully PCLD treatment was established (Krishna et al. 2007); The influence of the fluid-load on the cylindrical shell in the Bessel function was considered and the nature frequencies and loss factors of a fluid-filled cylindrical shell with PCLD treatment was discussed. A new general motion equation of the PCLD laminated structure by Hamilton principle and Donnell-Mushtari- Vlasov (DMV) assumption was reformulated (Hu et al. 2000). However, different from previous work, their equation only contained three displacement components, therefore its computational efficiency was improved greatly. Although FEM is simple and powerful to analyze the dynamic characteristics of the PCLD cylindrical shell with or without fluid-load, its accuracy is limited to low frequency range due to the adaptation of the low order interpolation function. Meanwhile, FEM is very time consuming when a large or complicated structure is computed. On the other hand, analytical methods for PCLD cylindrical shells are not always available due to its complex and arbitrary boundary conditions. After formulating the motion equation, an analytical solution for the axisymmetric vibration of a circular cylindrical shell with full PCLD treatment was obtained (Pan. 1969). By using the analysis method, the dynamic property of PCLD cylindrical shell has been computed (Cao et al. 2011). Therefore, semi-analytical methods for the PCLD cylindrical shells are further put forward such as assume mode method, modal strain energy method and transfer matrix method. Based on the Donnell thin shell theory and Hamilton principle, the motion equation and boundary conditions of the cylindrical shell with partial PCLD treatment was derived and the state space equation was constructed (Li et al. 2007). The vibration and damping characteristics of the PCLD cylindrical shell with clamped support condition at two ends is investigated by using transfer matrix method. However, the state vector in this approach was formulated by displacement components and their high order derivatives, thus the stress boundary conditions need to be expressed by the displacement components in advance, which was not easy and convenient to apply directly. Recently, a novel control equation of the PCLD cylindrical shell has been formulated and a transfer matrix method combined with highly precise extended homogeneous capacity precision integration technology has been proposed (Xiang et al. 2008). This method can be applied conveniently to the cylindrical shells with partial PCLD treatment under various boundary conditions. The state vector is formulated by the displacement and internal force components of the host shell and CL and provides a new means for the analysis of PCLD cylindrical shell. In order to enhance the vibration energy dissipation of the cylindrical shell with conventional PCLD treatment, the influence of multilayer PCLD treatment on vibration and noise suppression of the cylindrical shell loaded with liquid was investigated and analyzed (Saravanan et al. 2000).

This article applied the transfer function method to the dynamic analysis of multi-layer PCLD cylindrical shell. Based on the Donnell assumptions and linear visco-elastic theory, the constitutive relations for the five-layer PCLD cylindrical shell can be described. In terms of energy, the motion equations and boundary conditions are derived for the five-layer PCLD cylindrical shell by Hamilton principle. After trigonometric series expansion and Laplace transform, the state vector is introduced and the motion equation in state space is established. Then the state equation is solved by the transfer function method. Comparing with the traditional three-layer PCLD cylindrical shell, the results reveal that multi-layer PCLD cylindrical shell is more effective than the traditional three-layer PCLD cylindrical shell in suppressing vibration.

2. The constitutive relations

Figure 1 shows the geometry and coordinate system of five-layer PCLD cylindrical shell which was composed of the host shell (layer1), the VEM layers (layer 2 and layer 4) and the constrained layers (layer 3 and layer 5). x coordinate is in the axial direction of the shell, θ and the z coordinates are in the circumferential and radial directions of the shell respectively. R_i ($i=1,2,3,4,5$) denotes the middle surface radius of each layer; h_i denotes the thickness of each layer; and L denotes the length of the cylindrical shell.

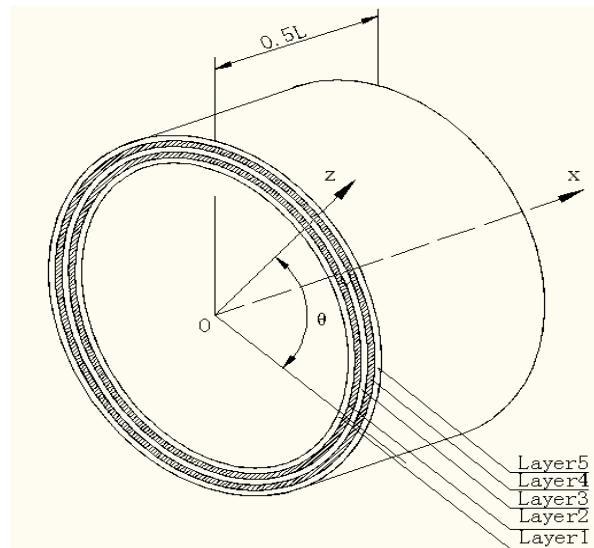


Figure 1. Geometry and coordinate system of five-layer PCLD cylindrical shell

To simplify the computational effort, the following assumptions are proposed (Li et al. 2008): 1) The extrusion deformation in z direction is negligible, that is, all layers have the same displacement in z direction; 2) There is no slip at the interfaces between layers, that is, perfect continuity; 3) The VEM undergoes only shear strains; 4) The host shell and constrained layers satisfy Kirchhoff's thin shell hypothesis and their shear strains were ignored; 5) all the cross-section moment of inertias are neglected; 6) all VEM's vibration inertias except the radial were neglected.

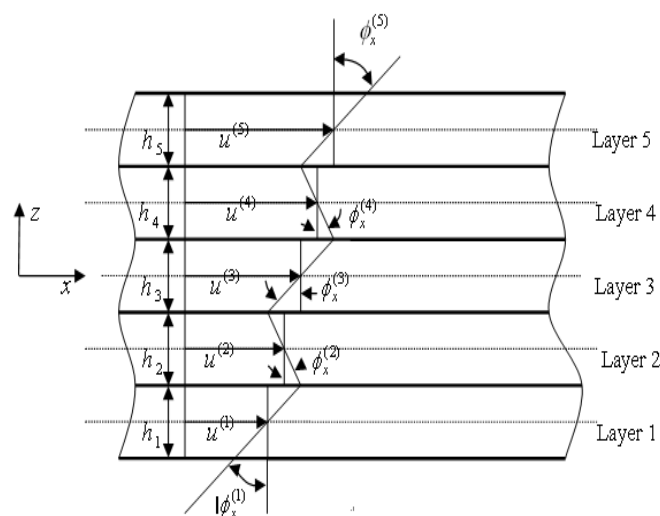


Figure 2. The deformation compatibility between layers

2.1. Displacements

Figure 2 shows the deformation compatibility between layers, the displacements of five-layer PCLD cylindrical shell can be written as

$$\begin{cases} \bar{u}^{(i)} = u^{(i)} + z\phi_x^{(i)} \\ \bar{v}^{(i)} = v^{(i)} + z\phi_\theta^{(i)} \end{cases} \quad i = 1, 2, 3, 4, 5 \quad (1)$$

Where the $u^{(i)}$ and $v^{(i)}$ denote the middle surface displacement amplitudes of the i^{th} layer in the x and θ directions respectively; the w is the displacement amplitude in the z direction; the $\phi_x^{(i)}$ and $\phi_\theta^{(i)}$ are rotation angles of the i^{th} layer around the x and θ coordinates respectively.

Based on the thin shell hypothesis, the following relationships are obtained

$$\begin{cases} \phi_x^{(1)} = \phi_x^{(3)} = \phi_x^{(5)} = -\frac{\partial w}{\partial x} \\ \phi_\theta^{(1)} = -\frac{\partial w}{R_1 \partial \theta} \\ \phi_\theta^{(3)} = -\frac{\partial w}{R_3 \partial \theta} \\ \phi_\theta^{(5)} = -\frac{\partial w}{R_5 \partial \theta} \end{cases} \quad (2)$$

By using the displacement continuity between layers, the following relationships are yielded

$$\begin{cases} u^{(2)} = \frac{1}{2}(u^{(1)} + \frac{h_1}{2}\phi_x^{(1)} + u^{(3)} - \frac{h_3}{2}\phi_x^{(3)}) \\ \phi_x^{(2)} = \frac{1}{h_2}(u^{(3)} - \frac{h_3}{2}\phi_x^{(3)} - u^{(1)} - \frac{h_1}{2}\phi_x^{(1)}) \\ v^{(2)} = \frac{1}{2}(v^{(1)} + \frac{h_1}{2}\phi_\theta^{(1)} + v^{(3)} - \frac{h_3}{2}\phi_\theta^{(3)}) \\ \phi_\theta^{(2)} = \frac{1}{h_2}(v^{(3)} - \frac{h_3}{2}\phi_\theta^{(3)} - v^{(1)} - \frac{h_1}{2}\phi_\theta^{(1)}) \end{cases} \quad (3)$$

$$\begin{cases} u^{(4)} = \frac{1}{2}(u^{(3)} + \frac{h_3}{2}\phi_x^{(3)} + u^{(5)} - \frac{h_5}{2}\phi_x^{(5)}) \\ \phi_x^{(4)} = \frac{1}{h_4}(u^{(5)} - \frac{h_5}{2}\phi_x^{(5)} - u^{(3)} - \frac{h_3}{2}\phi_x^{(3)}) \\ v^{(4)} = \frac{1}{2}(v^{(3)} + \frac{h_3}{2}\phi_\theta^{(3)} + v^{(5)} - \frac{h_5}{2}\phi_\theta^{(5)}) \\ \phi_\theta^{(4)} = \frac{1}{h_4}(v^{(5)} - \frac{h_5}{2}\phi_\theta^{(5)} - v^{(3)} - \frac{h_3}{2}\phi_\theta^{(3)}) \end{cases} \quad (4)$$

2.2. Strains

Based on the Kirchhoff's thin shell hypothesis, the middle surface strains of the host shell and constrained layers can be written as

$$\begin{cases} \varepsilon_{xx}^{o(i)} = \frac{\partial u^{(i)}}{\partial x} \\ \varepsilon_{\theta\theta}^{o(i)} = \frac{\partial v^{(i)}}{R_i \partial \theta} + \frac{w}{R_i} \\ \varepsilon_{x\theta}^{o(i)} = \frac{\partial v}{\partial x} + \frac{\partial u^{(i)}}{R_i \partial \theta} \end{cases} \quad i = 1, 3, 5 \quad (5)$$

On the other hand, the middle surface curvatures of the host shell and constrained layers can also be written as

$$\begin{cases} \kappa_{xx}^{(i)} = -\frac{\partial^2 w}{\partial x^2} \\ \kappa_{\theta\theta}^{(i)} = -\frac{1}{R_i^2} \frac{\partial^2 w}{\partial \theta^2} \\ \kappa_{x\theta}^{(i)} = -\frac{2}{R_i} \frac{\partial^2 w}{\partial x \partial \theta} \end{cases} \quad i = 1, 3, 5 \quad (6)$$

The strains of the host shell and constrained layers can be further derived

$$\begin{cases} \varepsilon_{xx}^{(i)} = \varepsilon_{xx}^{o(i)} + z\kappa_{xx}^{(i)} \\ \varepsilon_{\theta\theta}^{(i)} = \varepsilon_{\theta\theta}^{o(i)} + z\kappa_{\theta\theta}^{(i)} \\ \varepsilon_{x\theta}^{(i)} = \varepsilon_{x\theta}^{o(i)} + z\kappa_{x\theta}^{(i)} \end{cases} \quad i = 1, 3, 5 \quad (7)$$

The strains of VEM layers can be obtained

$$\begin{cases} \varepsilon_{xz}^{(2)} = \frac{\partial w}{\partial x} + \phi_x^{(2)} \\ \varepsilon_{\theta z}^{(2)} = \frac{1}{R_2} \frac{\partial w}{\partial \theta} - \frac{(v^{(2)} + z\phi_{\theta}^{(2)})}{R_2} + \phi_{\theta}^{(2)} \end{cases} \quad (8)$$

$$\begin{cases} \varepsilon_{xz}^{(4)} = \frac{\partial w}{\partial x} + \phi_x^{(4)} \\ \varepsilon_{\theta z}^{(4)} = \frac{1}{R_4} \frac{\partial w}{\partial \theta} - \frac{(v^{(4)} + z\phi_{\theta}^{(4)})}{R_4} + \phi_{\theta}^{(4)} \end{cases} \quad (9)$$

Substituted Eq.(3) and Eq.(4) into Eq.(8) and Eq.(9), and assuming $\frac{z}{R_2} \approx 0$ and $\frac{z}{R_4} \approx 0$ for the thin shell, the following relationships can be derived

$$\begin{cases} \varepsilon_{xz}^{(2)} = \frac{1}{h_2}(u_3 - u_1) + p_{x2} \frac{\partial w}{\partial x} \\ \varepsilon_{\theta z}^{(2)} = \left(\frac{1}{h_2} - \frac{1}{2R_2}\right)v_3 + \left(\frac{1}{h_2} + \frac{1}{2R_2}\right)v_1 \\ \quad + p_{\theta 2} \frac{\partial w}{\partial \theta} \end{cases} \quad (10)$$

$$\begin{cases} \varepsilon_{xz}^{(4)} = \frac{1}{h_4}(u_5 - u_3) + p_{x4} \frac{\partial w}{\partial x} \\ \varepsilon_{\theta z}^{(4)} = \left(\frac{1}{h_4} - \frac{1}{2R_4}\right)v_5 + \left(\frac{1}{h_4} + \frac{1}{2R_4}\right)v_3 \\ \quad + p_{\theta 4} \frac{\partial w}{\partial \theta} \end{cases} \quad (11)$$

Where, some geometric relationships are applied

$$\begin{aligned} p_{x2} &= \frac{1}{2h_2}(h_1 + 2h_2 + h_3) \\ p_{\theta 2} &= \frac{h_3}{2h_2R_3} + \frac{h_1}{2h_2R_1} + \frac{h_1}{2R_1R_2} - \frac{h_3}{2R_2R_3} + \frac{1}{R_2} \\ p_{x4} &= \frac{1}{2h_4}(h_3 + 2h_4 + h_5) \\ p_{\theta 4} &= \frac{h_5}{2h_4R_5} + \frac{h_3}{2h_4R_3} + \frac{h_3}{2R_3R_4} - \frac{h_5}{2R_4R_5} + \frac{1}{R_4} \end{aligned}$$

2.3. Stresses

Using the Hooke's Law, the stresses of the host shell and constrained layers are obtained

$$\begin{bmatrix} \sigma_{xx}^{(i)} \\ \sigma_{\theta\theta}^{(i)} \\ \sigma_{x\theta}^{(i)} \end{bmatrix} = \begin{bmatrix} Q_{11} & Q_{12} & 0 \\ Q_{12} & Q_{22} & 0 \\ 0 & 0 & Q_{66} \end{bmatrix} \begin{bmatrix} \varepsilon_{xx}^{(i)} \\ \varepsilon_{\theta\theta}^{(i)} \\ \varepsilon_{x\theta}^{(i)} \end{bmatrix} \quad i = 1, 3, 5 \quad (12)$$

Where, $Q_{11} = Q_{22} = \frac{E_i}{1 - \mu_i^2}$, $Q_{12} = \frac{E_i \mu_i}{1 - \mu_i^2}$, $Q_{66} = \frac{E_i}{2(1 + \mu_i)}$, E_i and μ_i denote the elastic modulus and poisson ratio of the i^{th} layer's material respectively. The shear stresses of VEM layers can be written as

$$\sigma_{xz}^{(2)} = G_2 \varepsilon_{xz}^{(2)} \quad \sigma_{\theta z}^{(2)} = G_2 \varepsilon_{\theta z}^{(2)} \quad (13)$$

$$\sigma_{xz}^{(4)} = G_4 \varepsilon_{xz}^{(4)} \quad \sigma_{\theta z}^{(4)} = G_4 \varepsilon_{\theta z}^{(4)} \quad (14)$$

Where, G_2 and G_4 are the complex shear modulus of VEM layers in 2nd and 4th layers, respectively.

3. Equations of motion

The strain energy of the host shell can be written as

$$\begin{aligned} U_1 &= \frac{1}{2} \iiint (\sigma_{xx}^{(1)} \varepsilon_{xx}^{(1)} + \sigma_{\theta\theta}^{(1)} \varepsilon_{\theta\theta}^{(1)} + \sigma_{x\theta}^{(1)} \varepsilon_{x\theta}^{(1)}) R_1 dz d\theta dx \\ &= \frac{1}{2} \iint K_1 [(\varepsilon_{xx}^{o(1)} + \varepsilon_{\theta\theta}^{o(1)})^2 - 2(1 - \mu_1)(\varepsilon_{xx}^{o(1)} \varepsilon_{\theta\theta}^{o(1)} - \\ &\quad \frac{\varepsilon_{x\theta}^{o(1)^2}}{4})] R_1 d\theta dx + \frac{1}{2} \iint D_1 [(\kappa_{xx}^{(1)} + \kappa_{\theta\theta}^{(1)})^2 \\ &\quad - 2(1 - \mu_1)(\kappa_{xx}^{(1)} \kappa_{\theta\theta}^{(1)} - \frac{\kappa_{x\theta}^{(1)^2}}{4})] R_1 d\theta dx \end{aligned} \quad (15)$$

where, $K_1 = \frac{E_1 h_1}{1 - \mu_1^2}$, $D_1 = \frac{E_1 h_1^3}{12(1 - \mu_1^2)}$. Replacing the subscript “1” with “3” and “5”, the strain energies

of two constrained layers U_3 and U_5 can be written in the same formula as Eq.(15) respectively.

The strain energies of the VEM layers can be written as

$$\begin{aligned} U_2 &= \frac{1}{2} \iiint (\sigma_{xz}^{(2)} \varepsilon_{xz}^{(2)} + \sigma_{\theta z}^{(2)} \varepsilon_{\theta z}^{(2)}) R_2 dz d\theta dx \\ &= \frac{R_2 G_2 h_2}{2} \iint (\varepsilon_{xz}^{(2)^2} + \varepsilon_{\theta z}^{(2)^2}) d\theta dx \end{aligned} \quad (16)$$

$$\begin{aligned} U_4 &= \frac{1}{2} \iiint (\sigma_{xz}^{(4)} \varepsilon_{xz}^{(4)} + \sigma_{\theta z}^{(4)} \varepsilon_{\theta z}^{(4)}) R_4 dz d\theta dx \\ &= \frac{R_4 G_4 h_4}{2} \iint (\varepsilon_{xz}^{(4)^2} + \varepsilon_{\theta z}^{(4)^2}) d\theta dx \end{aligned} \quad (17)$$

Therefore, the total strain energy of five-layer PCLD cylindrical shell is expressed by

$$U = U_1 + U_2 + U_3 + U_4 + U_5 \quad (18)$$

Taking the assumption (6) into consideration, the total kinetic energy is generated

$$\begin{aligned} T &= \frac{1}{2} \iint [m_1 R_1 (\dot{u}_1^2 + \dot{v}_1^2 + \dot{w}^2) + m_2 R_2 \dot{w}^2 + \\ &\quad m_3 R_3 (\dot{u}_3^2 + \dot{v}_3^2 + \dot{w}^2) + m_4 R_4 \dot{w}^2 + \\ &\quad m_5 R_5 (\dot{u}_5^2 + \dot{v}_5^2 + \dot{w}^2)] d\theta dx \end{aligned} \quad (19)$$

If the distributed load $q(x, \theta, t)$ is applied on the host shell, the virtual work from the distributed load is yield

$$\delta W = R_1 \iint q(x, \theta, t) \delta w d\theta dx \quad (20)$$

According to the Hamilton's principle: $\int_{t_0}^{t_1} (\delta U - \delta W - \delta T) dt = 0$, simplifying the motion equations

by $\frac{R_j}{R_i} \approx 1$, $1 \pm \frac{h_j}{2R_i} \approx 1$, then the motion equations of five-layer PCLD cylindrical shell can be derived

$$\begin{aligned}
m_1 \ddot{u}_1 - K_1 \left(\frac{\partial^2 u_1}{\partial x^2} + \frac{1+\mu_1}{2R_1} \frac{\partial^2 v_1}{\partial \theta \partial x} + \frac{\mu_1}{R_1} \frac{\partial w}{\partial x} + \frac{1-\mu_1}{2R_1^2} \frac{\partial^2 u_1}{\partial \theta^2} \right) - G_2 \varepsilon_{xz}^{(2)} &= 0 \\
m_1 \ddot{v}_1 - K_1 \left(\frac{1}{R_1^2} \frac{\partial^2 v_1}{\partial \theta^2} + \frac{1+\mu_1}{2R_1} \frac{\partial^2 u_1}{\partial \theta \partial x} + \frac{1}{R_1^2} \frac{\partial w}{\partial \theta} + \frac{1-\mu_1}{2} \frac{\partial^2 v_1}{\partial x^2} \right) - G_2 \varepsilon_{\theta z}^{(2)} &= 0 \\
m_3 \ddot{u}_3 - K_3 \left(\frac{\partial^2 u_3}{\partial x^2} + \frac{1+\mu_3}{2R_3} \frac{\partial^2 v_3}{\partial \theta \partial x} + \frac{\mu_3}{R_3} \frac{\partial w}{\partial x} + \frac{1-\mu_3}{2R_3^2} \frac{\partial^2 u_3}{\partial \theta^2} \right) + G_2 \varepsilon_{xz}^{(2)} - G_4 \varepsilon_{xz}^{(4)} &= 0 \\
m_3 \ddot{v}_3 - K_3 \left(\frac{1}{R_3^2} \frac{\partial^2 v_3}{\partial \theta^2} + \frac{1+\mu_3}{2R_3} \frac{\partial^2 u_3}{\partial \theta \partial x} + \frac{1}{R_3^2} \frac{\partial w}{\partial \theta} + \frac{1-\mu_3}{2} \frac{\partial^2 v_3}{\partial x^2} \right) + G_2 \varepsilon_{\theta z}^{(2)} - G_4 \varepsilon_{\theta z}^{(4)} &= 0 \\
m_5 \ddot{u}_5 - K_5 \left(\frac{\partial^2 u_5}{\partial x^2} + \frac{1+\mu_5}{2R_5} \frac{\partial^2 v_5}{\partial \theta \partial x} + \frac{\mu_5}{R_5} \frac{\partial w}{\partial x} + \frac{1-\mu_5}{2R_5^2} \frac{\partial^2 u_5}{\partial \theta^2} \right) + G_4 \varepsilon_{xz}^{(4)} &= 0 \\
m_5 \ddot{v}_5 - K_5 \left(\frac{1}{R_5^2} \frac{\partial^2 v_5}{\partial \theta^2} + \frac{1+\mu_5}{2R_5} \frac{\partial^2 u_5}{\partial \theta \partial x} + \frac{1}{R_5^2} \frac{\partial w}{\partial \theta} + \frac{1-\mu_5}{2} \frac{\partial^2 v_5}{\partial x^2} \right) + G_4 \varepsilon_{\theta z}^{(4)} &= 0 \\
m \ddot{w} + K_1 \left(\frac{w}{R_1^2} + \frac{1}{R_1^2} \frac{\partial v_1}{\partial \theta} + \frac{\mu_1}{R_1} \frac{\partial u_1}{\partial x} \right) + K_3 \left(\frac{w}{R_3^2} + \frac{1}{R_3^2} \frac{\partial v_3}{\partial \theta} + \frac{\mu_3}{R_3} \frac{\partial u_3}{\partial x} \right) + \\
K_5 \left(\frac{w}{R_5^2} + \frac{1}{R_5^2} \frac{\partial v_5}{\partial \theta} + \frac{\mu_5}{R_5} \frac{\partial u_5}{\partial x} \right) + D_1 \left(\frac{\partial^4 w}{\partial x^4} + \frac{1}{R_1^2} \frac{\partial^4 w}{\partial \theta^2 \partial x^2} + \frac{1}{R_1^4} \frac{\partial^4 w}{\partial \theta^4} \right) + \\
D_3 \left(\frac{\partial^4 w}{\partial x^4} + \frac{1}{R_3^2} \frac{\partial^4 w}{\partial \theta^2 \partial x^2} + \frac{1}{R_3^4} \frac{\partial^4 w}{\partial \theta^4} \right) + D_5 \left(\frac{\partial^4 w}{\partial x^4} + \frac{1}{R_5^2} \frac{\partial^4 w}{\partial \theta^2 \partial x^2} + \frac{1}{R_5^4} \frac{\partial^4 w}{\partial \theta^4} \right) - \\
G_2 h_2 (p_{x2} \frac{\partial \varepsilon_{xz}^{(2)}}{\partial x} + p_{\theta 2} \frac{\partial \varepsilon_{\theta z}^{(2)}}{\partial \theta}) - G_4 h_4 (p_{x4} \frac{\partial \varepsilon_{xz}^{(4)}}{\partial x} + p_{\theta 4} \frac{\partial \varepsilon_{\theta z}^{(4)}}{\partial \theta}) - q(x, \theta, t) &= 0
\end{aligned} \tag{21}$$

Here, $m=m_1+m_2+m_3+m_4+m_5$. Boundary conditions of clamped-clamped cylindrical shell at $x=-0.5L$ and $x=0.5L$ are further given by

$$\begin{aligned}
u_1 = 0 \quad \text{or} \quad N_{x1} &= K_1 \left(\frac{\partial u_1}{\partial x} + \frac{\mu_1}{R_1} \frac{\partial v_1}{\partial \theta} + \frac{\mu_1}{R_1} w \right) = 0 \\
v_1 = 0 \quad \text{or} \quad N_{x\theta 1} &= K_1 \frac{1-\mu_1}{2} \left(\frac{\partial v_1}{\partial x} + \frac{1}{R_1} \frac{\partial u_1}{\partial \theta} \right) = 0 \\
u_3 = 0 \quad \text{or} \quad N_{x3} &= K_3 \left(\frac{\partial u_3}{\partial x} + \frac{\mu_3}{R_3} \frac{\partial v_3}{\partial \theta} + \frac{\mu_3}{R_3} w \right) = 0 \\
v_3 = 0 \quad \text{or} \quad N_{x\theta 3} &= K_3 \frac{1-\mu_3}{2} \left(\frac{\partial v_3}{\partial x} + \frac{1}{R_3} \frac{\partial u_3}{\partial \theta} \right) = 0 \\
u_5 = 0 \quad \text{or} \quad N_{x5} &= K_5 \left(\frac{\partial u_5}{\partial x} + \frac{\mu_5}{R_5} \frac{\partial v_5}{\partial \theta} + \frac{\mu_5}{R_5} w \right) = 0 \\
v_5 = 0 \quad \text{or} \quad N_{x\theta 5} &= K_5 \frac{1-\mu_5}{2} \left(\frac{\partial v_5}{\partial x} + \frac{1}{R_5} \frac{\partial u_5}{\partial \theta} \right) = 0 \\
\frac{\partial w}{\partial x} = 0 \quad \text{or} \quad M_x &= D_1 \left(\frac{\partial^2 w}{\partial x^2} + \frac{\mu_1}{R_1^2} \frac{\partial^2 w}{\partial \theta^2} \right) + D_3 \left(\frac{\partial^2 w}{\partial x^2} \right. \\
&\quad \left. + \frac{\mu_3}{R_3^2} \frac{\partial^2 w}{\partial \theta^2} \right) + D_5 \left(\frac{\partial^2 w}{\partial x^2} + \frac{\mu_5}{R_5^2} \frac{\partial^2 w}{\partial \theta^2} \right) = 0 \\
w = 0 \quad \text{or} \quad Q_x &= D_1 \left(\frac{\partial^3 w}{\partial x^3} + \frac{2-\mu_1}{R_1^2} \frac{\partial^3 w}{\partial x \partial \theta^2} \right) + D_3 \left(\frac{\partial^3 w}{\partial x^3} \right. \\
&\quad \left. + \frac{2-\mu_3}{R_3^2} \frac{\partial^3 w}{\partial x \partial \theta^2} \right) + D_5 \left(\frac{\partial^3 w}{\partial x^3} + \frac{2-\mu_5}{R_5^2} \frac{\partial^3 w}{\partial x \partial \theta^2} \right) \\
&\quad - G_2 h_2 p_{x2} \varepsilon_{xz}^{(2)} - G_4 h_4 p_{x4} \varepsilon_{xz}^{(4)} = 0
\end{aligned} \tag{22}$$

For the isotropic PCLD cylindrical shells, the following formulas based on Fourier series are introduced to simplify the computed process

$$\begin{aligned}
u_1 &= \sum_{n=0}^{\infty} U_{1n}(x, t) \cos n\theta \quad v_1 = \sum_{n=0}^{\infty} V_{1n}(x, t) \sin n\theta \\
u_3 &= \sum_{n=0}^{\infty} U_{3n}(x, t) \cos n\theta \quad v_3 = \sum_{n=0}^{\infty} V_{3n}(x, t) \sin n\theta \\
u_5 &= \sum_{n=0}^{\infty} U_{5n}(x, t) \cos n\theta \quad v_5 = \sum_{n=0}^{\infty} V_{5n}(x, t) \sin n\theta \\
w &= \sum_{n=0}^{\infty} W_n(x, t) \cos n\theta \quad q = \sum_{n=0}^{\infty} q_n(x, t) \cos n\theta
\end{aligned} \tag{23}$$

where n denotes the circumferential wave number.

Substituting Eq.(23) into Eq.(21), and then Laplace transformation is made for Eq.(21). The following state equations in Laplace domain are yielded

$$\begin{aligned}
 \frac{\partial^2 \tilde{U}_{1n}}{\partial x^2} &= A_{u_1^u} \tilde{U}_{1n} + A_{v_1^v} \frac{\partial \tilde{V}_{1n}}{\partial x} + A_{u_3^u} \tilde{U}_{3n} + A_{w^u} \frac{\partial \tilde{W}_n}{\partial x} \\
 \frac{\partial^2 \tilde{V}_{1n}}{\partial x^2} &= A_{v_1^v} \frac{\partial \tilde{U}_{1n}}{\partial x} + A_{v_1^0} \tilde{V}_{1n} + A_{v_3^0} \tilde{V}_{3n} + A_{w^0} \tilde{W}_n \\
 \frac{\partial^2 \tilde{U}_{3n}}{\partial x^2} &= A_{u_3^u} \tilde{U}_{1n} + A_{u_3^u} \tilde{U}_{3n} + A_{v_3^v} \frac{\partial \tilde{V}_{3n}}{\partial x} + A_{u_5^u} \tilde{U}_{5n} + A_{w^u} \frac{\partial \tilde{W}_n}{\partial x} \\
 \frac{\partial^2 \tilde{V}_{3n}}{\partial x^2} &= A_{v_3^v} \tilde{V}_{1n} + A_{v_3^v} \frac{\partial \tilde{U}_{3n}}{\partial x} + A_{v_3^0} \tilde{V}_{3n} + A_{v_5^0} \tilde{V}_{5n} + A_{w^0} \tilde{W}_n \\
 \frac{\partial^2 \tilde{U}_{5n}}{\partial x^2} &= A_{u_5^u} \tilde{U}_{3n} + A_{u_5^u} \tilde{U}_{5n} + A_{v_5^v} \frac{\partial \tilde{V}_{5n}}{\partial x} + A_{w^u} \frac{\partial \tilde{W}_n}{\partial x} \\
 \frac{\partial^2 \tilde{V}_{5n}}{\partial x^2} &= A_{v_5^v} \tilde{V}_{3n} + A_{v_5^v} \frac{\partial \tilde{U}_{5n}}{\partial x} + A_{v_5^0} \tilde{V}_{5n} + A_{w^0} \tilde{W}_n \\
 \frac{\partial^4 \tilde{W}_n}{\partial x^4} &= A_{u_1^w} \frac{\partial \tilde{U}_{1n}}{\partial x} + A_{v_1^w} \tilde{V}_{1n} + A_{u_3^w} \frac{\partial \tilde{U}_{3n}}{\partial x} + A_{v_3^w} \tilde{V}_{3n} + A_{u_5^w} \frac{\partial \tilde{U}_{5n}}{\partial x} \\
 &\quad + A_{v_5^w} \tilde{V}_{5n} + A_{w^w} \tilde{W}_n + A_{w^w} \frac{\partial^2 \tilde{W}_n}{\partial x^2} + \tilde{f}^w
 \end{aligned} \tag{24}$$

All relevant coefficients in Eq.(24) are presented in appendix A.

Similarly, the boundary condition in Laplace domain can be derived

$$\begin{aligned}
 \tilde{U}_{1n} &= 0 \quad \text{or} \quad \tilde{N}_{x1} = K_1 \left(\frac{\partial \tilde{U}_{1n}}{\partial x} + \frac{\mu_1}{R_1} n \tilde{V}_{1n} + \frac{\mu_1}{R_1} \tilde{W}_n \right) = 0 \\
 \tilde{V}_{1n} &= 0 \quad \text{or} \quad \tilde{N}_{x\theta 1} = K_1 \frac{1-\mu_1}{2} \left(\frac{\partial \tilde{V}_{1n}}{\partial x} - \frac{n}{R_1} \tilde{U}_{1n} \right) = 0 \\
 \tilde{U}_{3n} &= 0 \quad \text{or} \quad \tilde{N}_{x3} = K_3 \left(\frac{\partial \tilde{U}_{3n}}{\partial x} + \frac{\mu_3}{R_3} n \tilde{V}_{3n} + \frac{\mu_3}{R_3} \tilde{W}_n \right) = 0 \\
 \tilde{V}_{3n} &= 0 \quad \text{or} \quad \tilde{N}_{x\theta 3} = K_3 \frac{1-\mu_3}{2} \left(\frac{\partial \tilde{V}_{3n}}{\partial x} - \frac{n}{R_3} \tilde{U}_{3n} \right) = 0 \\
 \tilde{U}_{5n} &= 0 \quad \text{or} \quad \tilde{N}_{x5} = K_5 \left(\frac{\partial \tilde{U}_{5n}}{\partial x} + \frac{\mu_5}{R_5} n \tilde{V}_{5n} + \frac{\mu_5}{R_5} \tilde{W}_n \right) = 0 \\
 \tilde{V}_{5n} &= 0 \quad \text{or} \quad \tilde{N}_{x\theta 5} = K_5 \frac{1-\mu_5}{2} \left(\frac{\partial \tilde{V}_{5n}}{\partial x} - \frac{n}{R_5} \tilde{U}_{5n} \right) = 0 \\
 \frac{\partial \tilde{W}_n}{\partial x} &= 0 \quad \text{or} \quad \tilde{M}_x = (D_1 + D_3 + D_5) \frac{\partial^2 \tilde{W}_n}{\partial x^2} - (D_1 \frac{\mu_1}{R_1^2} \\
 &\quad + D_3 \frac{\mu_3}{R_3^2} + D_5 \frac{\mu_5}{R_5^2}) n^2 \tilde{W}_n = 0 \\
 \tilde{W}_n &= 0 \quad \text{or} \quad \tilde{Q}_x = (D_1 + D_3 + D_5) \frac{\partial^3 \tilde{W}_n}{\partial x^3} - \left[\frac{n^2 D_1 (2-\mu_1)}{R_1^2} \right. \\
 &\quad \left. + \frac{n^2 D_3 (2-\mu_3)}{R_3^2} + \frac{n^2 D_5 (2-\mu_5)}{R_5^2} + G_2 h_2 p_{x2}^2 + G_4 h_4 p \right] \tilde{W}_n = 0
 \end{aligned} \tag{25}$$

4. Transfer function method

In order to solve Eq.(24), the state vector is defined as follows

$$\tilde{\beta}_n = \left\{ \tilde{U}_{1n}, \frac{\partial \tilde{U}_{1n}}{\partial x}, \tilde{V}_{1n}, \frac{\partial \tilde{V}_{1n}}{\partial x}, \tilde{U}_{3n}, \frac{\partial \tilde{U}_{3n}}{\partial x}, \tilde{V}_{3n}, \frac{\partial \tilde{V}_{3n}}{\partial x}, \tilde{U}_{5n}, \frac{\partial \tilde{U}_{5n}}{\partial x}, \tilde{V}_{5n}, \frac{\partial \tilde{V}_{5n}}{\partial x}, \tilde{W}_n, \frac{\partial \tilde{W}_n}{\partial x}, \frac{\partial^2 \tilde{W}_n}{\partial x^2}, \frac{\partial^3 \tilde{W}_n}{\partial x^3} \right\}^T$$

In this way, Eq.(24) can be written as

$$\frac{\partial}{\partial x} \tilde{\beta}_n(x, s) = B_n(s) \tilde{\beta}_n(x, s) + \tilde{f}_n(x, s) \tag{26}$$

Where, $B_n(s)$ and $\tilde{f}_n(x, s)$ are presented in appendix B.

For clamped-clamped five-layer PCLD cylindrical shell, the boundary conditions can be expressed by

$$P_n \tilde{\beta}_n(-0.5L, s) + Q_n \tilde{\beta}_n(0.5L, s) = 0 \quad (27)$$

Where, $P_n = \begin{bmatrix} \Lambda \\ 0_{8 \times 16} \end{bmatrix}$, $Q_n = \begin{bmatrix} 0_{8 \times 16} \\ \Lambda \end{bmatrix}$,

$$\Lambda = \begin{bmatrix} 1 & 0 & 0 & 0 & 0 & 0 & 0 & 0 & 0 & 0 & 0 & 0 & 0 & 0 & 0 & 0 \\ 0 & 0 & 1 & 0 & 0 & 0 & 0 & 0 & 0 & 0 & 0 & 0 & 0 & 0 & 0 & 0 \\ 0 & 0 & 0 & 0 & 1 & 0 & 0 & 0 & 0 & 0 & 0 & 0 & 0 & 0 & 0 & 0 \\ 0 & 0 & 0 & 0 & 0 & 0 & 1 & 0 & 0 & 0 & 0 & 0 & 0 & 0 & 0 & 0 \\ 0 & 0 & 0 & 0 & 0 & 0 & 0 & 0 & 1 & 0 & 0 & 0 & 0 & 0 & 0 & 0 \\ 0 & 0 & 0 & 0 & 0 & 0 & 0 & 0 & 0 & 0 & 1 & 0 & 0 & 0 & 0 & 0 \\ 0 & 0 & 0 & 0 & 0 & 0 & 0 & 0 & 0 & 0 & 0 & 0 & 1 & 0 & 0 & 0 \\ 0 & 0 & 0 & 0 & 0 & 0 & 0 & 0 & 0 & 0 & 0 & 0 & 0 & 0 & 1 & 0 & 0 \end{bmatrix}.$$

The solution of Eq.(26) can be written as

$$\tilde{\beta}_n = \int_{-0.5L}^{0.5L} D_n(x, \xi, s) \tilde{f}_n(\xi, s) d\xi \quad (28)$$

Where, $D_n(x, \xi, s) = \begin{cases} e^{B_n(s)} [P_n e^{-0.5LB_n(s)} + Q_n e^{0.5LB_n(s)}]^{-1} P_n e^{B_n(s)(-0.5L-\xi)}, & \xi \leq x \\ -e^{B_n(s)} [P_n e^{-0.5LB_n(s)} + Q_n e^{0.5LB_n(s)}]^{-1} Q_n e^{B_n(s)(0.5L-\xi)}, & \xi > x \end{cases}$

By solving the characteristic equation

$$\det[P_n e^{-0.5LB_n(s)} + Q_n e^{0.5LB_n(s)}] = 0 \quad (29)$$

natural frequency and loss factor of five-layer PCLD cylindrical shell can be obtained. All the derived processes and solving approach for the five-layer PCLD cylindrical shell can be extended to seven-layer and even more layer PCLD cylindrical shells.

5. Numerical results and analysis

5.1. The five-layer PCLD cylindrical shell

The geometric and physical properties of five-layer PCLD cylindrical shell are presented as following:

$R_1=0.3\text{m}$, $L=0.1\text{m}$, $h_1=0.003\text{m}$, $h_2=0.0005\text{m}$, $h_3=0.001\text{m}$, $h_4=0.0005\text{m}$, $h_5=0.001\text{m}$,

$G_2=G_4=0.896(1+0.9683i)\text{Mpa}$, $\mu_1=\mu_3=\mu_5=0.3$, $\mu_2=\mu_4=0.498$, $\rho_1=\rho_3=\rho_5=2700\text{kg}/\text{m}^3$

$\rho_2=\rho_4=999\text{kg}/\text{m}^3$.

The boundary condition is the clamped-clamped.

Table 1. Comparison of TFM with ANSYS for five-layer PCLD cylindrical shell

N	Natural frequency (Hz)			Loss factor (%)		
	TFM	ANSYS	error (%)	TFM	ANSYS	error (%)
0	2975	2976	0.034	0.357	0.359	0.560
1	2942	2943	0.034	0.367	0.369	0.545
2	2850	2851	0.035	0.398	0.398	0.000
3	2723	2725	0.073	0.450	0.448	0.444
4	2588	2589	0.039	0.523	0.520	0.574
5	2458	2461	0.122	0.617	0.612	0.810
6	2350	2353	0.128	0.728	0.721	0.962
7	2265	2270	0.221	0.851	0.844	0.822
8	2208	2214	0.272	0.980	0.972	0.816
9	2180	2186	0.275	1.104	1.099	0.453
10	2180	2186	0.275	1.216	1.214	0.164

Table 1 shows the natural frequency and loss factor calculated by the proposed transfer function method and commercial finite element analysis software ANSYS. The maximum error of natural

frequency and loss factor are 0.275% and 0.962% respectively. Compared to ANSYS approach, the transfer function method needs less process variables and computational cost.

5.2. Multilayer PCLD cylindrical shell

The above five-layer PCLD cylindrical shell can be extended to multilayer PCLD cylindrical shell, while keeping the thickness of the host shell and the total thickness of VEM layers and the total thickness of constrained layers unchanged such as seven-layer, nine-layer and even more layers PCLD cylindrical shell.

Table 2. Natural frequency and loss factor for multilayer PCLD cylindrical shell

n	Natural frequency (Hz)					Loss factor (%)				
	3	5	7	9	11	3	5	7	9	11
0	3029	2975	2966	2964	2963	0.249	0.357	0.422	0.475	0.520
1	2996	2941	2930	2930	2929	0.256	0.367	0.435	0.488	0.535
2	2907	2849	2840	2837	2836	0.276	0.398	0.470	0.529	0.579
3	2784	2723	2712	2710	2709	0.311	0.450	0.532	0.597	0.654
4	2658	2586	2575	2572	2570	0.360	0.523	0.618	0.694	0.759
5	2532	2458	2445	2441	2440	0.421	0.617	0.730	0.819	0.896
6	2431	2348	2334	2330	2329	0.492	0.728	0.862	0.967	1.056
7	2357	2264	2249	2444	2242	0.569	0.851	1.010	1.134	1.250
8	2311	2208	2190	2185	2183	0.648	0.980	1.165	1.309	1.430
9	2295	2180	2160	2154	2150	0.722	1.104	1.317	1.481	1.618
10	2307	2179	2157	2150	2148	0.785	1.216	1.454	1.637	1.790
11	2347	2206	2181	2173	2171	0.835	1.307	1.568	1.767	1.935
12	2415	2258	1230	2222	2219	0.869	1.373	1.651	1.864	2.043
13	2508	2335	2305	2295	2292	0.886	1.412	1.702	1.924	2.110
14	2625	2436	2402	2392	2388	0.887	1.425	1.722	1.948	2.140
15	2766	2559	2522	2510	2506	0.876	1.416	1.713	1.941	2.135
16	2928	2703	2662	2649	2645	0.854	1.388	1.683	1.909	2.101
17	3111	2867	2882	2820	2803	0.826	1.347	1.635	1.850	2.046
18	3315	3049	3000	2996	2979	0.792	1.296	1.575	1.766	1.974
19	3537	3250	3197	3197	3173	0.755	1.240	1.508	1.698	1.894
20	3777	3467	3410	3390	3384	0.718	1.180	1.437	1.630	1.807

Table 2 shows the natural frequency and loss factor for multilayer PCLD cylindrical shell by using transfer function method. It is noted that the natural frequency decreases slightly while the loss factor increases obviously when the layer number is increased, it is special obvious when the circumferential wave number is around 13. Furthermore, when more PCLD layers are bonded to the surface of the host shell while keeping the total thickness of VEM and the total thickness of CL unchanged, the natural frequency decreases or the loss factor increases in a smaller amount with the total layer number increasing.

In order to check the vibration response of multilayer PCLD cylindrical shell, a distributed force $q(x, \theta, t) = \delta(t) \cos(n\theta) Pa$ is applied on the inner side of host shell. Based on the orthogonality of trigonometric function, the steady-state response is sinusoidal with n waves. In this article, we only compute the radial vibration at point (0, 0, 0.3). Figure 3-Figure 5 show the displacement amplitude-frequency response curves for multilayer PCLD cylindrical shell when wave number n is 6, 14 and 20. It is obvious that when the total layer number increases, the peak of curve decreases significantly. The natural frequency around the peak is corresponding with the natural frequency shown in table 2 when the circumferential wave number n is 6, 14, 20 respectively. On the other hand, when the total layer number increases, the natural frequency around the peak decreases rapidly at the beginning and slowly at the end. That means more layers of PCLD will result in much less decrease in the natural frequency of multilayer PCLD cylindrical shell. Meanwhile, it is further proved theoretically that multilayer

PCLD treatment will increase the loss factor significantly, thus enhance the vibration energy dissipation and suppress the vibration and noise of structures. It supplies an effective means to suppress the vibration and noise of structures without extra VEM and CL material.

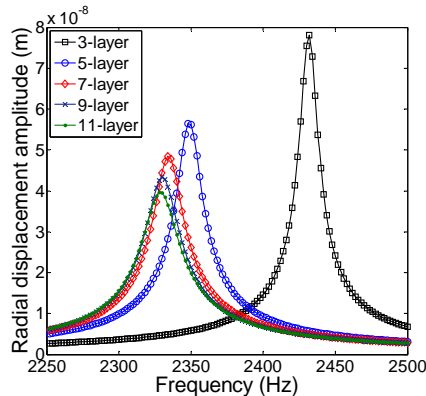


Figure 3. Displacement frequency response for $n=6$

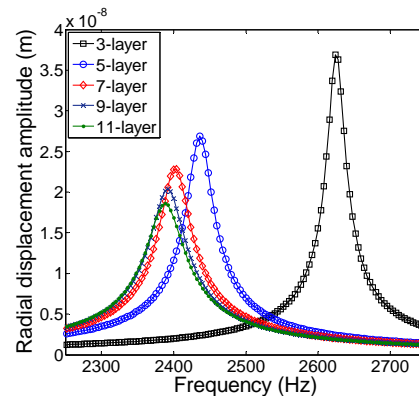


Figure 4. Displacement frequency response for $n=14$

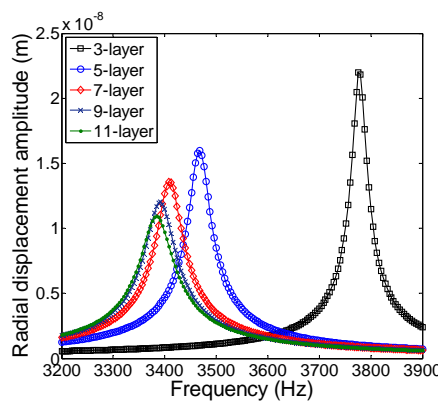


Figure 5. Displacement frequency response for $n=20$

6. Conclusions

The constitutive relations of the cylindrical shell with five-layer PCLD treatment are described based on the Donnell theory of thin shell. The Hamilton principle is used to derive the motion equation of the cylindrical shell with five-layer PCLD treatment. The state vectors are defined and the state space form of the motion equation is further constructed to solve the motion equation conveniently. The transfer matrix method is applied to solve the state space equation. The natural frequency and the loss factor of the cylindrical shell with conventional three-layer and multilayer PCLD treatments are calculated. The results are concluded as follows:

(1) The application of multilayer PCLD treatment results in a slight drop of natural frequency and a rapid increase in loss factor. Therefore, it supplies an effective means to enhance vibration energy dissipation of the cylindrical shell without extra VEM and CL material applied.

(2) The theoretical analysis in this paper is an important fundamental to push forward the application of multilayer PCLD treatments as a practical, economical and effective means in structural vibration suppression. However, there are still more works to do in this topic, such as the optimization of the layer number, the selection of parameters as well as the layout of PCLD patches. Therefore, the multi-objective optimization will be further considered as an effective design tool to maximize vibration energy dissipation of the cylindrical shell with multilayer PCLD treatment.

Appendix A

$$\begin{aligned}
A_{u_1^0}^{u_1} &= \left[\frac{K_1 n^2 (1 - \mu_1)}{2R_1^2} + \frac{G_2}{h_2} + m_1 s^2 \right] / K_1, \quad A_{v_1^1}^{u_1} = \left[-\frac{K_1 n (1 + \mu_1)}{2R_1} \right] / K_1, \quad A_{u_3^0}^{u_1} = \left(-\frac{G_2}{h_2} \right) / K_1, \\
A_{w^1}^{u_1} &= -\left(\frac{K_1 \mu_1}{R_1} + G_2 p_x \right) / K_1, \quad A_{u_1^1}^{v_1} = \frac{K_1 n (1 + \mu_1)}{2R_1} / \left[\frac{K_1 (1 - \mu_1)}{2} \right], \\
A_{v_1^0}^{v_1} &= \left[\frac{K_1 n^2}{R_1^2} + G_2 \left(\frac{1}{h_2} + \frac{1}{2R_2} \right) + m_1 s^2 \right] / \left[\frac{K_1 (1 - \mu_1)}{2} \right], \quad A_{v_3^0}^{v_1} = -G_2 \left(\frac{1}{h_2} - \frac{1}{2R_2} \right) / \left[\frac{K_1 (1 - \mu_1)}{2} \right], \\
A_{w^0}^{v_1} &= \left(\frac{nK_1}{R_1^2} + G_2 p_\theta n \right) / \left[\frac{K_1 (1 - \mu_1)}{2} \right], \quad A_{u_1^0}^{u_3} = -\left(\frac{G_2}{h_2} \right) / K_3, \quad A_{v_1^1}^{u_3} = \left[-\frac{K_3 n (1 + \mu_3)}{2R_3} \right] / K_3, \\
A_{u_3^0}^{u_3} &= \left[\frac{K_3 n^2 (1 - \mu_3)}{2R_3^2} + \frac{G_2}{h_2} + m_3 s^2 \right] / K_3, \quad A_{w^1}^{u_3} = \left(G_2 p_x - \frac{K_3 \mu_3}{R_3} \right) / K_3, \quad A_{v_1^0}^{v_3} = -G_2 \left(\frac{1}{h_2} + \frac{1}{2R_2} \right) / \left[\frac{K_3 (1 - \mu_3)}{2} \right], \\
A_{u_3^1}^{v_3} &= \frac{K_3 n (1 + \mu_3)}{2R_3} / \left[\frac{K_3 (1 - \mu_3)}{2} \right], \quad A_{v_3^0}^{v_3} = \left[\frac{K_3 n^2}{R_3^2} + G_2 \left(\frac{1}{h_2} - \frac{1}{2R_2} \right) + m_3 s^2 \right] / \left[\frac{K_3 (1 - \mu_3)}{2} \right], \\
A_{w^0}^{v_3} &= \left(\frac{nK_3}{R_3^2} - G_2 p_\theta n \right) / \left[\frac{K_3 (1 - \mu_3)}{2} \right], \quad A_{u_1^1}^w = -\left(\frac{K_1 \mu_1}{R_1} + G_2 p_x \right) / (D_1 + D_3), \\
A_{v_1^0}^w &= -\left(\frac{K_1 n}{R_1^2} + G_2 p_\theta n \right) / (D_1 + D_3), \quad A_{u_3^1}^w = -\left(\frac{K_3 \mu_3}{R_3} - G_2 p_x \right) / (D_1 + D_3), \quad A_{v_3^0}^w = -\left(\frac{K_3 n}{R_3^2} - G_2 p_\theta n \right) / (D_1 + D_3), \\
A_{w^0}^w &= -\left[\left(\frac{D_1}{R_1^4} + \frac{D_3}{R_3^4} \right) n^4 + \frac{K_1}{R_1^2} + \frac{K_3}{R_3^2} + G_2 h_2 p_\theta^2 n^2 + m s^2 \right] / (D_1 + D_3), \\
A_{w^1}^w &= \left[2 \left(\frac{D_1}{R_1^4} + \frac{D_3}{R_3^4} \right) n^2 + G_2 h_2 p_x^2 \right] / (D_1 + D_3), \quad \tilde{f}^w = \tilde{q}_n / (D_1 + D_3 + D_5)
\end{aligned}$$

Appendix B

$$B_n(s) = \begin{bmatrix}
0 & 1 & 0 & 0 & 0 & 0 & 0 & 0 & 0 & 0 & 0 & 0 & 0 & 0 & 0 \\
A_{u_1^0}^{u_1} & 0 & 0 & A_{v_1^1}^{u_1} & A_{u_3^0}^{u_1} & 0 & 0 & 0 & 0 & 0 & 0 & 0 & 0 & A_{w^1}^{u_1} & 0 \\
0 & 0 & 0 & 1 & 0 & 0 & 0 & 0 & 0 & 0 & 0 & 0 & 0 & 0 & 0 \\
0 & A_{u_1^1}^{v_1} & A_{v_1^0}^{v_1} & 0 & 0 & 0 & A_{v_1^0}^{v_3} & 0 & 0 & 0 & 0 & 0 & A_{w^0}^{v_1} & 0 & 0 \\
0 & 0 & 0 & 0 & 0 & 1 & 0 & 0 & 0 & 0 & 0 & 0 & 0 & 0 & 0 \\
A_{u_1^0}^{u_3} & 0 & 0 & 0 & A_{u_3^1}^{u_3} & 0 & 0 & A_{v_1^1}^{u_3} & A_{u_3^0}^{u_3} & 0 & 0 & 0 & 0 & A_{w^1}^{u_3} & 0 \\
0 & 0 & 0 & 0 & 0 & 0 & 0 & 1 & 0 & 0 & 0 & 0 & 0 & 0 & 0 \\
0 & 0 & A_{v_1^0}^{v_3} & 0 & 0 & A_{u_3^1}^{v_3} & A_{v_3^0}^{v_3} & 0 & 0 & 0 & A_{v_3^1}^{v_3} & 0 & A_{w^0}^{v_3} & 0 & 0 \\
0 & 0 & 0 & 0 & 0 & 0 & 0 & 0 & 1 & 0 & 0 & 0 & 0 & 0 & 0 \\
0 & 0 & 0 & 0 & A_{u_3^0}^{u_3} & 0 & 0 & 0 & A_{v_1^0}^{u_3} & 0 & 0 & A_{v_3^0}^{u_3} & 0 & A_{w^0}^{u_3} & 0 \\
0 & 0 & 0 & 0 & 0 & 0 & 0 & 0 & 0 & 0 & 1 & 0 & 0 & 0 & 0 \\
0 & 0 & 0 & 0 & 0 & 0 & A_{v_3^0}^{v_3} & 0 & 0 & A_{v_3^1}^{v_3} & A_{v_3^0}^{v_3} & 0 & A_{w^0}^{v_3} & 0 & 0 \\
0 & 0 & 0 & 0 & 0 & 0 & 0 & 0 & 0 & 0 & 0 & 0 & 1 & 0 & 0 \\
0 & 0 & 0 & 0 & 0 & 0 & 0 & 0 & 0 & 0 & 0 & 0 & 0 & 1 & 0 \\
0 & 0 & 0 & 0 & 0 & 0 & 0 & 0 & 0 & 0 & 0 & 0 & 0 & 0 & 1 \\
0 & A_{u_1^1}^w & A_{v_1^0}^w & 0 & 0 & A_{u_3^1}^w & A_{v_3^0}^w & 0 & 0 & A_{u_3^0}^w & A_{v_3^1}^w & 0 & A_{w^0}^w & 0 & A_{w^1}^w
\end{bmatrix}$$

$$\tilde{f}_n(x, s) = \left\{ 0 \quad 0 \quad 0 \quad 0 \quad 0 \quad 0 \quad 0 \quad 0 \quad 0 \quad 0 \quad 0 \quad 0 \quad 0 \quad 0 \quad 0 \quad \tilde{f}^w \right\}^T$$

References

- [1] Kerwin E M 1959 *J. Acoust. Soc. Am.* **31** 952-62
- [2] Mead D J and Markus S 1969 *AIAA Journal*. **10** 163-75
- [3] Yeh J Y and Chen L W 2006 *Compos. Struct.* **73** 53-60
- [4] Zhang Q J and Sainsbury M G 2000 *Comput. Struct.* **74** 717-30
- [5] Chen Y C and Huang S C 2002 *Int. J. Mech. Sci.* **44** 1801-21
- [6] Ramesh T C and Ganesan N 1994 *J. Sound. Vib.* **171** 577-601
- [7] Ramesh T C and Ganesan N 1994 *J. Sound. Vib.* **175** 535-55
- [8] Ramesh T C and Ganesan N 1994 *J. Sound. Vib.* **175** 359-70

- [9] Wang H J and Chen L W 2004 *Finite Elem. Anal. Des.* **40** 737-55
- [10] Krishna B V and Ganesan N 2007 *J. Sound. Vib.* **303** 575-95
- [11] Hu Y C and Huang S C 2000 *J. Comput. Struct.* **16** 577- 91
- [12] Pan H H 1969 *J. Sound Vib.* **9** 338-48
- [13] Cao X T, Zhang Z I and Hua H X 2011 *Appl. Math. Mech.* **32** 495-506
- [14] Li E Q, Li D K, Tang G J and Lei Y J 2007 *Acta Aeronaut. Et Astronaut. Sin.* **28** 1487-93
- [15] Xiang Y, Huang Y Y and Lu J 2008 *Appl. Math. Mech.* **29** 1587-600
- [16] Saravanan C, Ganesan N and Ramamurti.V 2000 *Comput. Struct.* **75** 395-417
- [17] Li E Q, Li D K and Tang G.J 2008 *Eng. Mech.* **25** 6-11